Design Dialogue Journal

Analyzing the Effects of Shear Deformations on the Constrained Observability Method

Seyyedbehrad Emadi [1]*

[1] DICIV, Department of Civil Engineering, University of Salerno, Fisciano (SA), Italy.

* Correspondence: behradei@gmail.com

Abstract: In the traditional observability method, due to the linearity of the system of equations, measurement sets must usually include redundant measurements. This feature might be especially problematic in those structures where numerous measurements are not possible. To solve this problem and to increase its applicability, the constrained observability method was recently presented. One of the main controversial features of this procedure is that as most of the structural system identification methods, this technique is based on the Euler-Bernoulli beam theory, therefore shear deformation effects are neglected in its formulation. Nevertheless, in a number of structures such as deep beams, when actual deformations on-site are considered to estimate the mechanical properties of the elements, neglecting shear deformation effects can result in serious errors in the properties observed. To fill these gaps, after thorough bibliographic research, shear deformation is included in a Structural System Identification method (constrained observability analysis) and parametric analyses are carried out to evaluate the role that shear deformation plays in the structural behavior of structures with different slenderness ratios.

Keywords: Structural system identification, Structural analysis, Stiffness matrices method, Shear effects, Constraint observability method.

1. Introduction

Damages in structures usually produce changes in their structural behavior due to the changes made in mechanical properties. In order to identify the effects of these damages, Structural System Identification (SSI) might be used. This process is based on a subset of measured inputs and outputs (e.g. forces and/or displacements). Inputs can be simply obtained by non-destructive tests (the measured structural response under a certain load case). Based on the nature of the load, these tests might be categorized as static (see e.g. (Sanayei, M et al. (1996) and Abdo, M.A. (2012)) [1, 2] or dynamics (see e.g. Chao, et al. (2014) and Lin, K.C. et al. (2016)) [3, 4]. Also, SSI methods can be classified as a parametric [5, 6] or non-parametric methods [7, 8].

Parametric methods depend on the physical-based models, while in non-parametric ones, parameters do not have any physical meaning. In non-parametric methods, parameters are identified directly with optimization procedures that minimize the difference between the predicted structural response and the measured ones. For parametric SSI methods, a mathematical representation of the structural behavior is required. The most common way to do this modeling is based on the Stiffness Matrix Method (SMM) [9-12].

Received: 16 November 2024
Accepted: 09 December 2024
Published: 13 December 2024

The details of the main SSI methods proposed in the literature are presented in American Society of Civil Engineers, Reston, VA 2013 [13]. Matrix methods of structural analysis are universally accepted in structural design. Rapid and accurate analysis of complex structures is abled by these methods under both static and dynamic conditions. There are many studies related to different SMM methods (e.g. Zarga, D. et al (2019), López-Colina, C. et al (2019) Chao, S., et al (2019) [14-16]. Most of these studies are based on either Euler-Bernoulli's beam theory [17] or Timoshenko's beam theory [18].

As Euler-Bernoulli's beam theory approach is based on the plain section deformation assumption [19], shear deformations are neglected in this method. The only circumstances that this theory stands are the one which shear force is a constant bending moment alongside the beam. Although, due to the neglecting value of shear deformation in comparison with flexural ones, these effects can be overlooked. Nevertheless, in some structures (such as a deep beam) shear deformation effects can play an important role and lack considering them should be considered as a modeling error such as any other feature in the model assumed with a wrong value [20].

Timoshenko was the first one who include shear effects in the beam theory which is known as the Timoshenko beam theory or first order shear deformation theory [21]. In this theory, two different rotations are considered: rotation due to the bending, wb, and rotation due to the shear, wr. Besides bending rotation, shear rotation between the cross-section and the bending line is allowed in this method. The difference between the two methods in a simply supported beam is presented in Figure 1 (Euler-Bernoulli's beam theory Figure 1.b and Timoshenko's beam theory Figure 1.c).

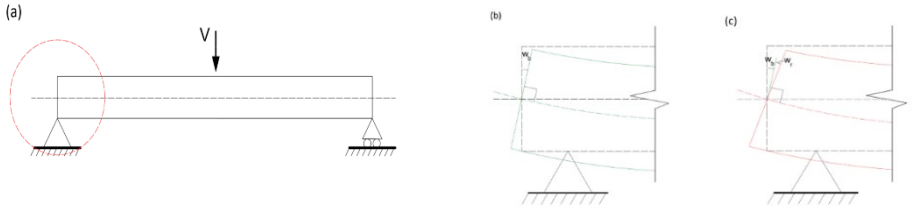

Figure 1. (a) A simply supported beam with a zoomed support. (b) Euler-Bernoulli's beam theory on the beam support. (c) Timoshenko's beam theory on the beam support.

2. Observability Method

One of the most common methods of the Finite Element Method (FEM) is the SMM. In 2D, for SMM based on the Euler-Bernoulli's beam theory, the elemental stiffness matrix [k] or tree degrees of freedom (two deflections (u and v) and one rotation (w) at the element node, beam element of length L and constant cross-section is:

$$k = \begin{bmatrix} \frac{EA}{L} & 0 & 0 \\ 0 & \frac{12EI}{L^3} & \frac{6EI}{L^2} \\ 0 & \frac{6EI}{L^2} & \frac{4EI}{L} \end{bmatrix} \quad (1)$$

Where E, A and I are Young modulus, area and inertia respectively. In static structural analysis, a statement of the equilibrium conditions together with the strength of materials theory leads to a relation between forces and displacements that has the form of a system of equations:

$$[K]\cdot\{\delta\}=\{f\} \quad (2)$$

Where the displacements vector {δ} contains the horizontal, vertical, and rotational displacements, the external force vector {f} contains the horizontal forces, vertical forces, and moments and the global stiffness matrix [K] contains the stiffness of the beam elements. According to the literature, in 1968, Przemieniecki (1968) modified SMM based on Timoshenko's beam theory for the very first time [22]. Stiffness matrix including shear stiffness is as follows:

$$[K]=\begin{bmatrix} \frac{EA}{L} & 0 & 0 & -\frac{EA}{L} & 0 & 0 \\ 0 & \frac{12EI}{L^3(1+\emptyset)} & \frac{6EI}{L^2(1+\emptyset)} & 0 & -\frac{12EI}{L^3(1+\emptyset)} & \frac{6EI}{L^2(1+\emptyset)} \\ 0 & \frac{6EI}{L^2(1+\emptyset)} & \frac{EI(4+\emptyset)}{L(1+\emptyset)} & 0 & -\frac{6EI}{L^2(1+\emptyset)} & \frac{EI(2-\emptyset)}{L(1+\emptyset)} \\ -\frac{EA}{L} & 0 & 0 & \frac{EA}{L} & 0 & 0 \\ 0 & -\frac{12EI}{L^3(1+\emptyset)} & -\frac{6EI}{L^2(1+\emptyset)} & 0 & \frac{12EI}{L^3(1+\emptyset)} & -\frac{6EI}{L^2(1+\emptyset)} \\ 0 & \frac{6EI}{L^2(1+\emptyset)} & \frac{EI(2-\emptyset)}{L(1+\emptyset)} & 0 & -\frac{6EI}{L^2(1+\emptyset)} & \frac{EI(4+\emptyset)}{L(1+\emptyset)} \end{bmatrix} \quad (3)$$

Unlike the traditional stiffness matrix, a coefficient Ø known as the shear parameter appears in some elements of Equation (3). This parameter is as follows:

$$\emptyset=\frac{12EI}{GA_vL^2}\ , \quad (4)$$

Where A_v is the shear area and G is the shear modulus. Also, the coefficient v is Poisson's ratio as shown in Eq. (5). In the denominator of most terms of Przemieniecki's stiffness matrix, the shear parameter Ø can be seen. To fix this problem, Tomas, D. et al. (2018) proposed the following change of variable implying a shear parameter Q [20]. This OM shear parameter is described as follows (Eq. (6)):

$$G=\frac{E}{2(1+v)}\ , \qquad Q=\frac{\emptyset}{1+\emptyset} \quad (5),(6)$$

By replacing the shear parameter Ø by OM shear parameter Q, the stiffness matrix can be upgraded to:

$$[K]=\begin{bmatrix} \frac{EA}{L} & 0 & 0 & -\frac{EA}{L} & 0 & 0 \\ 0 & \frac{12EI}{L^3}-\frac{12EIQ}{L^3} & \frac{6EI}{L^2}-\frac{6EIQ}{L^2} & 0 & -\frac{12EI}{L^3}+\frac{12EIQ}{L^3} & \frac{6EI}{L^2}-\frac{6EIQ}{L^2} \\ 0 & \frac{6EI}{L^2}-\frac{6EIQ}{L^2} & \frac{4EI}{L}-\frac{3EIQ}{L} & 0 & -\frac{6EI}{L^2}+\frac{6EIQ}{L^2} & \frac{2EI}{L}-\frac{3EIQ}{L} \\ -\frac{EA}{L} & 0 & 0 & \frac{EA}{L} & 0 & 0 \\ 0 & -\frac{12EI}{L^3}+\frac{12EIQ}{L^3} & -\frac{6EI}{L^2}+\frac{6EIQ}{L^2} & 0 & \frac{12EI}{L^3}-\frac{12EIQ}{L^3} & -\frac{6EI}{L^2}+\frac{6EIQ}{L^2} \\ 0 & \frac{6EI}{L^2}-\frac{6EIQ}{L^2} & \frac{2EI}{L}-\frac{3EIQ}{L} & 0 & -\frac{6EI}{L^2}+\frac{6EIQ}{L^2} & \frac{4EI}{L}-\frac{3EIQ}{L} \end{bmatrix} \quad (7)$$

Once, the boundary conditions, the applied nodal forces in a certain static load test and the geometry are defined, displacements can be measured to observe the unknown mechanical properties in the SMM. To do so, an inverse analysis is performed. The known information is clustered in a subset $\delta_1$and f_1 of $\{\delta\}$ and $\{f\}$, respectively and the subset δ_0 of $\{\delta\}$ and a subset f_0 of $\{f\}$ are assumed as unknown information. The equation (2) can be rewritten as follows:c

$$[K^*]\cdot\{\delta^*\}=\begin{bmatrix} K_{00}^* & K_{01}^* \\ K_{10}^* & K_{11}^* \end{bmatrix}\cdot\begin{Bmatrix} \delta_0^* \\ \delta_1^* \end{Bmatrix}=\begin{Bmatrix} f_0 \\ f_1 \end{Bmatrix}=\{f\}\ , \quad (8)$$

In order to collect the unknowns in the left-hand side and the knowns in the right-hand side, the Equation (8) is rearranged as:

$$[B]\cdot\{z\}=\begin{bmatrix}K_{10}^{*} & 0\\ K_{00}^{*} & -I\end{bmatrix}\cdot\begin{Bmatrix}\delta_{0}^{*}\\ f_{0}\end{Bmatrix}=\begin{Bmatrix}f_{1}-K_{11}^{*}\delta_{1}^{*}\\ -K_{01}^{*}\delta_{1}^{*}\end{Bmatrix}=\{D\}, \tag{9}$$

Where 0 and I are the null and the identity matrices, respectively. To check if the system has a solution, the null space $[V]$ of matrix $[B]$ should be calculated and check that $[V]^{T}\{D\}=0$. If the equation holds, the system is compatible; otherwise, it has no solution. The general solution (the set of all solutions) of the system (9) has the structure [23, 24]:

$$\{Z\}=\{Z_{\mathrm{p}}\}+[V]\cdot\{\rho\}, \tag{10}$$

Where $\{Z_{\mathrm{p}}\}$ is a particular solution of the system (10). $[V].\{\rho\}$ is the set of all solutions of the associated homogeneous system of equations (a linear space of solutions, where the columns of $[V]$ are a basis of this linear space and the elements of the vector $\{\rho\}$ are arbitrary real values that describe the coefficients of all possible linear combinations). It should be noted that a variable has a unique solution not only when the matrix $[V]$ has zero dimension (it does not exist), but when the associated row in the matrix $[V]$ is null. Thus, the examination of the matrix $[V]$ and identification of its null rows leads to the identification of the subset of variables with a unique solution in vector {Z}. It is interesting to note that if all parameters of vector {Z} are not observed from the null space, any deflection, force or parameter observed after the initial OM analysis will be used to observe new parameters by using a recursive process. For more information, readers are addressed to [5, 21, 25-30].

One of the main flaws of the OM is the linearization of the unknowns as products of unknowns are considered as new linear unknowns. This assumption might lead to a significant loss of information.

Lei et al. (2017) found that in OM, the nonlinear constraints among product variables are lacking. Based on his work, these observability method characteristics are due to the following reasons: (a) the immature end of the recursive steps and (b) the ineffective measurements because of redundancy in the measurement sets (the same problem appearing in example 1) [31]. By adding some nonlinear constraints to the OM procedure, the Constraint Observability Method (COM) solves the main OM's flaws: the value of the solution of the coupled unknowns has to be equal to the product of the single unknowns. Hence, the COM first includes nonlinear constraints and then solves the system of equations numerically. Therefore, it does not produce any symbolic solution. It is to say that OM provides a symbolic solution.

In this method, variables are categorized in one of the following three categories: (1) Coupled variables Vc (Iwj and Qwj from example 1); (2) Single variables Vs1 (I and Q from example 1), which already exist in the unknown {Z} vector; (3) Single variables Vs2 (wj from example 1), which did not exist in the unknown vector {Z} from OM. The new vector {Z} is named {Z*}, and it is a combination of vector {Z} and the new single variables Vs2. In order to create an objective function for a numerical optimization process, Eq. (9) can be rewritten as follow:

$$\{\in\}=[B^{*}]\cdot\{Z^{*}\}-\{D\}, \tag{11}$$

Where vector $\in$ is the residual of the equations which is a vector with the same number of rows of the original matrix [B] and $B^{*}=[B^{N_{eq}\times N_{z}}|\Omega^{N_{eq}\times N_{s2}}]$ is obtained by adding a null matrix Ω to the matrix B calculated from the last recursive step of SSI by OM. The size of this null matrix Ω is $N_{eq}\times N_{s2}$. N_{eq} and N_{z}, explain the number of equations and the

number of unknowns in {Z} respectively. N_{s2} explains the number of new single unknowns in Vs2.

The goal of the objective function is determined by minimizing the square sum of the residuals, {∈}. To reach a certain level of efficiency in the COM optimization process, variables of Eq. (10) should be normalized. The optimization toolbox of Matlab [32] has been used to obtain the optimal solution of the objective function. In order to limit the computational expenses and the time of the optimization process, the stopping criterion has to be defined. In order to reach a certain level of efficiency in the COM optimization process, variables of Eq. (11) can be normalized.

The algorithm for SSI by COM is summarized as follows:

- **Step 1**: Apply SSI by OM to analyze whether full observability is possible or not. If so, there is no need to apply COM, due to the more computational time in comparison with OM. If full observability is not possible, update the input of OM until no new unknowns are observable.
- **Step 2**: Obtain the equation (9) from the last step of the OM recursive process then generates the new unknown vector of Z* including Coupled variables Vc; as well as single variables Vs1 and Vs2.
- **Step 3**: Add a null matrix [Ω] to the matrix [B] to generate $[B^*]$, in order to contain Vs2 in Z* without violating the system.
- **Step 4**: Obtain the normalized unknown parameters.
- **Step 5**: Guess the initial values of unknown parameters of the Z* vector, set the bound for the solution and solve the optimization process to find the minimized value for the residual vector, ∈.

A summary of the procedure is shown in the flow chart in Figure 2. For more information about the COM, the reader is addressed to Lei.et al. (2017) [31].

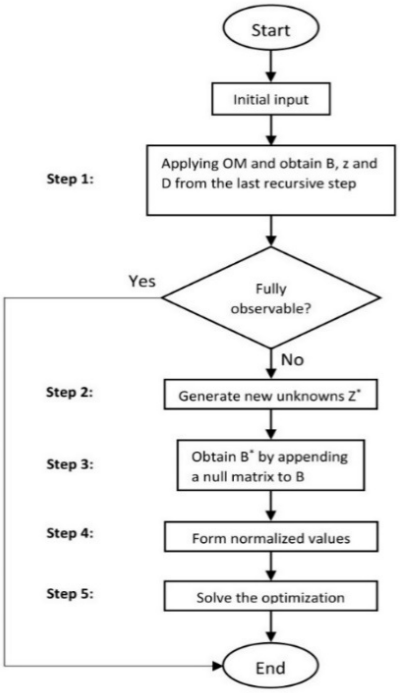

Fig. 2 Flow chart of structural system identification by COM [26]

The majority of SSI methods are based on the Euler-Bernoulli beam theory. Originally, the traditional COM method was not able to consider the effects of shear in measurements. Neglecting this deformation can be assumed as a modeling error, an error in the mathematical model. Emadi et al (2019) updated the equations to the procedure proposed for OM by Tomás et al. (2018) [20, 26]. With this new updated method, the problem of linearization in OM variables is solved and equations related to shear stiffnesses are taken into account. Therefore, now it is possible to evaluate the effects of neglecting shear deformation in traditional COM procedure since these effects were not considered in the formulation of the method. With this aim in the upcoming section, the effects of shear deformation are studied to show the important role that these effects can play in some structures.

3. Actual Vertical Deflection in Direct Analysis

For most structures, shear effects are usually much smaller than the flexural effects, so neglecting the shear deformation is not an important issue. However, deformation due to the shear might play an important role in some structures. In order to compare the effect of deformation due to bending and shear, a sensitivity analysis performs by a simply supported beam and a cantilever beam under the concentrated and uniform load, results are compared in different examples.

3.1 Example 1: simply supported beam with a concentrated load

Consider a simply supported beam with 3 nodes and 4 Timoshenko beam elements as shown in Fig. 3. Beam has a constant cross-section and the value of young modulus, Poisson ratio, shear area, cross-sectional area and inertia of all elements along the beam are constant. Young's modulus is $E = 27000\ MPa$ and Poisson's ratio is $v = 0.25$. beams have rectangular cross-sections 1 m deep ($h = 1\ m$) and 0.1 m wide ($b = 0.1\ m$), so the area is $A = 0.1\ m^2$ and the Inertia is $I = 0.008\ m^4$. The properties of this simply supported beam are listed in table 1. The boundary conditions of the structure are horizontal and vertical displacements restricted in node 1 and vertical displacement restricted in node 3 (this is to say, u1=v1=v3= 0) and the only external force applied is a concentrated vertical force in node 2 of 100kN (V2= 100kN).

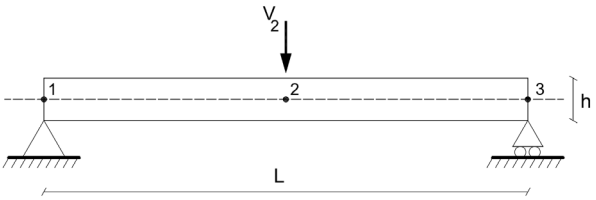

Figure 3. Example 1. FEM for a simply supported beam.

Table 1: Properties of the FEM of the simply supported beam.

Area [m^2]	0.100
Shear Area [m^2]	0.833
Inertia [m^4]	0.008
Young's Modulus [GPa]	27.000
Poisson's Ratio γ	0.250

In order to calculate the bending and shear deformation in the middle node of the structure in this academic example with different height to span ratio, formulations based on Timoshenko beam theory is used. The value of bending vertical deflections, v_b and shear vertical deflections v_s, in the node number 2 for the loading case is presented in Eq. (12), (13). To analyze the effect of the shear deflection at node number 2, a parametric analysis

is carried out. In this analysis, the length of the beam (L) varies from 0.1 to 10 meters while the height (h) remains constant. Fig. 4 illustrates how the slenderer beam, the lower the deformation is. As it is presented in Fig 4.a, the shape of the shear deflection variation is changing slowly when the ratio varies between1 to 10. In Fig 4.b, the ration between shear and bending deformation for different L/h ration are presented.

$$v_b = \frac{V_2 * L^3}{48 * E * I}\ ,\ v_s = \frac{V_2}{4 * A_v * G} * L\ , \qquad (12), (13)$$

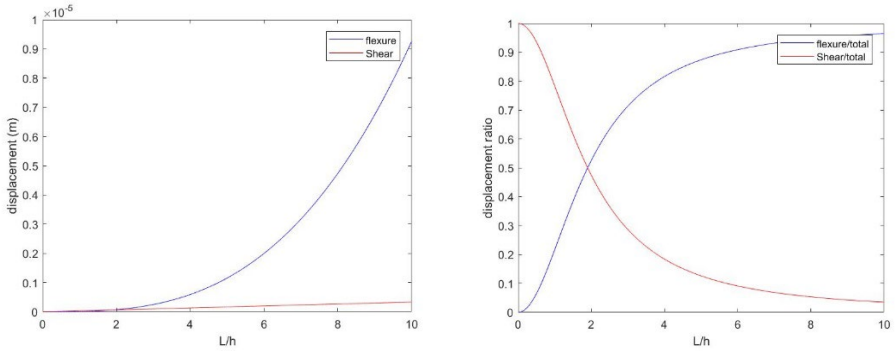

Figure 4: Example 1. (a) Deformation due to bending and shear at the node number 2. (b) The ratio between shear and bending deformation at Node 2.

In Fig. 4.b, the equal value of shear and bending deformation is gained when the ratio of L/h is 2. In addition, it is to say that the ratio of shear deformation varies from 0.99 to 0.03 where the length to height ratio is between 0.1 to 10. This analysis illustrates the shear deformation in not negligible in beams with a small span to deep ration, so neglecting of measuring the shear deformation, may cause errors in the estimation of structural parameters of structures.

3.2 Example 2: cantilever beam with a concentrated load

Consider a cantilever beam with the same properties and cross-section as in Example 1 modeled with a single beam element and two nodes as shown in Fig.5. Properties of this simply supported beam are listed in table 1. The boundary conditions of the structure are horizontal, vertical displacements and bending rotation are restricted in Node 1 (this is to say, u1=v1= wb1= 0) and the only external force applied is a concentrated vertical force in node 2 of 100kN (V2= 100kN).

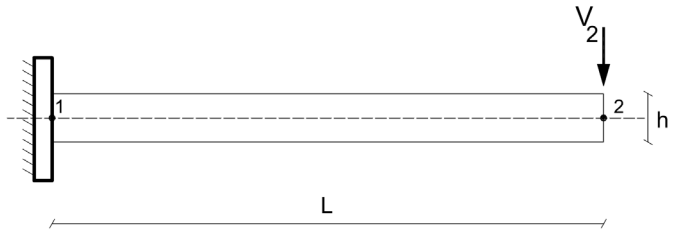

Figure 5. Example 2. FEM for a cantilever beam.

In order to calculate the bending and shear deformation in the node number 2 of the structure in this academic example with different height to span ratio, formulations based on Timoshenko beam theory is used. The value of bending vertical deflections, v_b and shear vertical deflections v_s, in the node number 2 for the loading case is presented in Eq. (14) and Eq. (15). To analyze the effect of the shear deflection at node number 2, a parametric analysis is carried out. In this analysis, the length of the beam (L) varies from

0.1 to 10 meters while the height (h) remains constant. Fig. 6 illustrates how the slenderer beam, the lower the deformation is. As it is presented in Fig 6.a, the shape of the shear deflection variation is changing slowly when the ratio between1 to 10 varying while the bending deformation growing faster than shear. In Fig 6.b, the ration between shear and bending deformation for different L/h ration are presented.

$$v_b = \frac{V_2 * L^3}{3 * E * I}\ ,\ v_s = \frac{V_2}{A_v * G} * L\ , \qquad (14), (15)$$

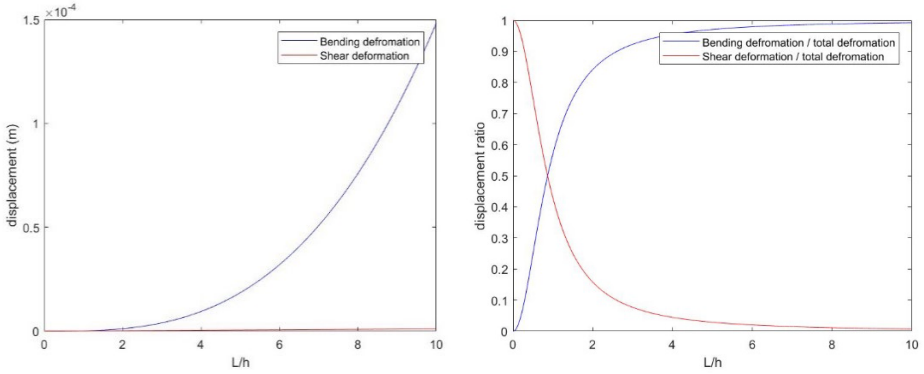

Figure 6: Example 2. (a) deformation due to bending and shear at the node number 2. (b) The ratio between shear and bending deformation at Node 2.

In Fig. 6.b, the equal value of shear and bending deformation is gained when the ratio of L/h is 1. In addition, it is to say that the ratio of shear deformation varies from 0.99 to 0.02 where the length to height ratio is between 0.1 to 10. This analysis illustrates the shear deformation in not negligible in beams with a small span to deep ration, so neglecting of measuring the shear deformation, may cause errors in the estimation of structural parameters of structures.

4. Actual Vertical Deflection in Inverse Analysis

Neglecting the shear deformation in the measured deflections may lead to significant errors in the inertia estimation by inverse analysis. A major concern in SSI methods in actual structures is related to the errors in measurements. As most SSI methods based on SMM are not able to consider the effects of shear, this phenomenon can lead to modeling errors. This is due to the fact that the vertical deflection on-site will not correspond with the one considered by the model (shear effects are neglected in the equations). Depending on the structure, these modeling errors can surpass measurement errors. These errors will appear even in noise-free measurements and they will affect the estimation of structural properties in SSI methods. To establish a guideline for different structural cases, a sensitivity analysis is developed in this section for the two previous structures (Example 1 and 2). In this analysis, the total vertical deflection (sum of shear and bending deflection) in different length to height ratio (1 to 10) is tested. The effects of these errors in estimating the inertia in different structural cases (simply supported beam of example 1 and cantilever beam of example 3) can be seen in Fig. 7. The results of these analyses illustrate the cases where the calculation of shear effects in SSI methods is important.

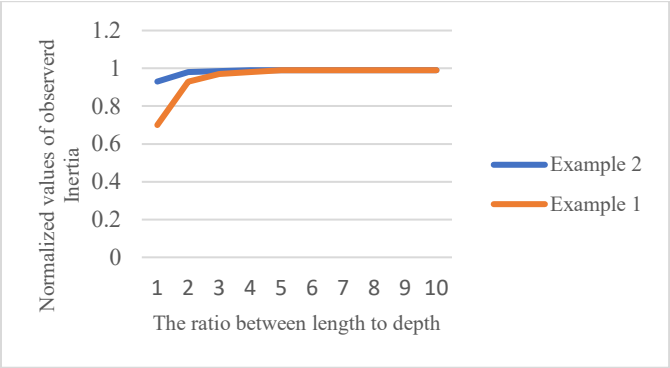

Figure 7. Normalized values of observed inertia when actual vertical deflections are taken into account based on the length-to-depth ratio in SSI methods.

Where the ratio of L/h is 3 (deep beam limitation by Eurocode EN) [33], the normalized value of estimated inertia (observed value divided by real value) for a simply supported beam and cantilever beams are 0.97 and 0.985 of real values, respectively. in addition, when the L/h ratio is 1, the normalized value of the estimation of inertia for a simply supported beam and the cantilever beams are 0.7 and 0.93, respectively. The results from Fig. 7 shows the fact that the effects of shear deformation on inverse analysis are even more important than in the direct one and these effects in the inverse analysis should not be neglected.

6. Conclusion

Structural System Identification (SSI) methods usually neglect deflections due to shear in their formulation as this phenomenon is usually less significant than the bending rotation. Despite the important role that this deflection might play in some structures, especially deep beams. To fill this gap, this paper presents the first study focused on analyzing these effects in the direct and inverse analysis. In order to show how important, the role of shear deformation might be, two different structures (a simply supported beam and a cantilever) with different length-to-height ratios are studied. In fact, these examples illustrate that the difference between Timoshenko's theory and Euler-Bernoulli's theory in terms of deflection is higher for members with low length-to-height ratio. Indeed, for deep beams ratio between the shear and bending deflection can be significant in favor of shear effects. For the first time in literature, the sensitivity of the SSI methods to this modeling error is performed. The study of this sensitivity analysis might provide some insight into which structures rotation due to shear should be taken into account and in which cases these effects can be neglected.

Acknowledgments

The authors are indebted to the Spanish Ministry of Economy and Competitiveness for the funding provided through the research project BIA2017-86811-C2-1-R directed by José Turmo and BIA2017-86811-C2-2-R. All these projects are funded with FEDER funds. The authors are also indebted to AGAUR for the funding provided through 2017 SGR 1481.

References

[1] Sanayei, M., & Saletnik, M. J. (1996). Parameter estimation of structures from static strain measurements I: Formulation. *Journal of Structural Engineering, 122*(6), 555–562. https://doi.org/10.1061/(ASCE)0733-9445(1996)122:5(555)

[2] Abdo, M. A. (2012). Parametric study of using only static response in structural damage detection. *Engineering Structures, 34*, 124–131. https://doi.org/10.1016/j.engstruct.2011.09.027

[3] Chao, S. H., & Loh, C. H. (2014). Application of singular spectrum analysis to structural monitoring and damage diagnosis of bridges. *Structure and Infrastructure Engineering, 10(6)*, 708–727. https://doi.org/10.1080/15732479.2012.758643

[4] Lin, K. C., Hung, H. H., & Sung, Y. C. (2016). Seismic performance of high-strength reinforced concrete buildings evaluated by nonlinear pushover and dynamic analyses. *International Journal of Structural Stability and Dynamics, 16(03)*, 1450107. https://doi.org/10.1142/S0219455414501077

[5] Lozano-Galant, J. A., Nogal, M., Castillo, E., & Turmo, J. (2013). Application of observability techniques to structural system identification. *Computer-Aided Civil and Infrastructure Engineering, 28*(6), 434–450. https://doi.org/10.1111/mice.12004

[6] Gracia-Palencia, A. J., Santini-Bell, E., Sipple, J. D., & Sanayei, M. (2015). Structural model updating of an in-service bridge using dynamic data. *Structural Control and Health Monitoring, 22*(10), 1265–1281. https://doi.org/10.1002/stc.1742

[7] Karabelivo, K., Cuéllar, P., Baebler, M., & Rucker, W. (2015). System identification of inverse, multimodal, and nonlinear problem using evolutionary computing: Application to a pile structure supported in nonlinear springs. *Engineering Structures, 101*, 609–620.

[8] Mei, L., Mita, A., & Zhou, J. (2016). An improved substructural damage detection approach of shear structure based on ARMAX model residual. *Structural Control and Health Monitoring, 23*(2), 218–236. https://doi.org/10.1002/stc.1766

[9] Hou, Z., Xia, H., Zhang, Y., Zhang, T., & Y, W. (2015). Dynamic analysis and model test on steel-concrete composite beams under moving loads. *Steel and Composite Structures, 18*(3), 565–582.

[10] Kahya, V., & Turan, M. (2018). Vibration and buckling of laminated beams by a multi-layer finite element model. *Steel and Composite Structures, 28*(4), 415–426. https://doi.org/10.12989/scs.2018.28.4.415

[11] Li, J., Huo, Q., Li, X., Kong, X., & Wu, W. (2014). Dynamic stiffness analysis of steel-concrete composite beams. *Steel and Composite Structures, 16*(6), 577–593. https://doi.org/10.12989/scs.2014.16.6.577

[12] Araki, Y., & Miyagi, Y. (2005). Mixed integer nonlinear least-squares problem for damage detection in truss structures. *Journal of Engineering Mechanics, 131*(7), 659–667. https://doi.org/10.1061/(ASCE)0733-9399(2005)131:7(659)

[13] American Society of Civil Engineers. (2013). *Structural identification of constructed systems*. Reston, VA: American Society of Civil Engineers.

[14] Zarga, D., Tounsi, A., Bousahla, A. A., Bourada, F., & Mahmoud, S. R. (2019). Thermomechanical bending study for functionally graded sandwich plates using a simple quasi-3D shear deformation theory. *Steel and Composite Structures, 32*(3), 389–410. https://doi.org/10.12989/scs.2019.32.3.389

[15] López-Colina, C., Serrano, M. A., Lozano, M., Gayarre, F. L., Suárez, J. M., & Wilkinson, T. (2019). Characterization of the main component of equal width welded I-beam-to-RHS-column connections. *Steel and Composite Structures, 32*(3), 337–346. https://doi.org/10.12989/scs.2019.32.3.337

[16] Chao, S., Wu, H., Zhou, T., Guo, T., & Wang, C. (2019). Application of self-centering wall panel with replaceable energy dissipation devices in steel frames. *Steel and Composite Structures, 32*(2), 265–279. https://doi.org/10.12989/scs.2019.32.2.265

[17] Kawano, A., & Zine, A. (2019). Reliability evaluation of continuous beam structures using data concerning the displacement of points in a small region. *Engineering Structures, 180*, 379–387. https://doi.org/10.1016/j.engstruct.2018.11.051

[18] Arefi, M., Pourjamshidian, M., & Ghorbanpour Arani, A. (2019). Dynamic instability region analysis of sandwich piezoelectric nano-beam with FG-CNTRCs face-sheets based on various high-order shear deformation and nonlocal strain gradient theory. *Steel and Composite Structures, 32*(2), 157–171. https://doi.org/10.12989/scs.2019.32.2.151

[19] Dahake, A., Ghugal, Y., & Kalwane, U. B. (2014). Displacements in thick beams using refined shear deformation theory. *Proceedings of the 3rd International Conference on Recent Trends in Engineering & Technology,* Tamil Nadu, India.

[20] Tomas, D., Lozano-Galant, J. A., Ramos, G., & Turmo, J. (2018). Structural system identification of thin web bridges by observability techniques considering shear deformation. *Thin-Walled Structures, 123*, 282–293. https://doi.org/10.1016/j.tws.2017.11.017

[21] Timoshenko, S. P. (1921). On the correction for shear of the differential equation for transverse vibrations of prismatic bars. *Philosophical Magazine, 41*(6), 742–746. https://doi.org/10.1080/14786442108636264

[22] Przemieniecki, J. S. (1968). *Theory of matrix structural analysis.* Library of Congress Catalog Card Number 67-19151.

[23] Castillo, E., Cobo, A., Jubete, F., Pruneda, R. E., & Castillo, C. (2000). An orthogonally based pivoting transformation of matrices and some applications. *SIAM Journal on Matrix Analysis and Applications, 22*(3), 666–681. https://doi.org/10.1137/S0895479898349720

[24] Castillo, E., Jubete, F., Pruneda, R. E., & Solares, C. (2002). Obtaining simultaneous solutions of linear subsystems of equations and inequalities. *Linear Algebra and its Applications, 364*(1–3), 131–154. https://doi.org/10.1016/S0024-3795(01)00500-6

[25] Lozano-Galant, J. A., Emadi, S., Ramos, G., & Turmo, J. (2018). Structural system identification of shear stiffnesses in beams by observability techniques. *40th IABSE Symposium Nantes 2018: Tomorrow's Megastructures* (pp. S24-111–S24-118). International Association for Bridge and Structural Engineers (IABSE).

[26] Emadi, S., & Collaborators. (2019). Structural system identification including shear deformation of composite bridges from vertical deflections. *Steel and Composite Structures, 32*(6), 731–741. https://doi.org/10.12989/scs.2019.32.6.731

[27] Emadi, S., & Emadi, S. (2022). Analyzing cost and time objectives in construction projects using artificial neural networks. *International Review of Civil Engineering (IRECE, 13*(2), 91–98. https://doi.org/10.15866/irece.v13i2.21124

[28] Emadi, S., & Collaborators. (2023). Simplified calculation of shear rotations for first-order shear deformation theory in deep bridge beams. *Applied Sciences (Switzerland, 13*(5), Article 3362. https://doi.org/10.3390/app13053362

[29] Emadi, S., Sun, Y., Lozano-Galant, J. A., & Turmo, J. (2023). Observing material properties in composite structures from actual rotations. *Applied Sciences, 13*(20), Article 11456. https://doi.org/10.3390/app132011456

[30] Lozano, F., & Collaborators. (2024). Enhancing performance evaluation of low-cost inclinometers for the long-term monitoring of buildings. *Journal of Building Engineering, 87*, Article 109148. https://doi.org/10.1016/j.jobe.2024.109148

[31] Lei, J., Nogal, M., Lozano-Galant, J.A., Xu, D., & Turmo, J. (2017). Constrained observability method in static structural system identification. *Struct. Control Health Monit*, 25(1), e2040. https://doi.org/10.1002/stc.2040

[32] MATLAB and Optimization Toolbox Release 2017b. (2017). *The MathWorks, Inc.*, Natick, Massachusetts, United States.

[33] CEN. (2002). *EN 1992-1-1: Eurocode 2: Design of concrete structures - Part 1-1: General rules and rules for buildings.* Brussels, Belgium: European Committee for Standardization.